

## Bisphenol A Promotes Human Prostate Stem-Progenitor Cell Self-Renewal and Increases In Vivo Carcinogenesis in Human Prostate Epithelium

Gail S. Prins, Wen-Yang Hu, Guang-Bin Shi, Dan-Ping Hu, Shyama Majumdar, Guannan Li, Ke Huang, Jason L. Nelles, Shuk-Mei Ho, Cheryl Lyn Walker, Andre Kajdacsy-Balla, and Richard B. van Breemen

Department of Urology (G.S.P., W.-Y.H., G.-B.S., D.-P.H., S.M., J.L.N.) and Department of Pathology (A.K.-B.), College of Medicine, and Department of Medicinal Chemistry and Pharmacognosy (G.L., K.H., R.B.v.B.), College of Pharmacy, University of Illinois at Chicago, Chicago, Illinois 60612; University of Illinois Cancer Center (G.S.P., A.K.B., R.B.v.B.), Chicago, Illinois 60612; Department of Environmental Health (S.-M.H.), University of Cincinnati, Cincinnati, Ohio 45220; and Center for Translational Cancer Research (C.L.W.), Institute of Biosciences and Technology, Texas A&M University System Health Science Center, College Station, Texas 77843

Previous studies in rodent models have shown that early-life exposure to bisphenol A (BPA) reprograms the prostate and enhances its susceptibility to hormonal carcinogenesis with aging. To determine whether the human prostate is similarly sensitive to BPA, the current study used human prostate epithelial stem-like cells cultured from prostates of young, disease-free donors. Similar to estradiol-17 $\beta$  (E<sub>2</sub>), BPA increased stem-progenitor cell self-renewal and expression of stem-related genes in a dose-dependent manner. Further, 10 nM BPA and E<sub>2</sub> possessed equimolar membrane-initiated signaling with robust induction of p-Akt and p-Erk at 15 minutes. To assess in vivo carcinogenicity, human prostate stem-progenitor cells combined with rat mesenchyme were grown as renal grafts in nude mice, forming normal human prostate epithelium at 1 month. Developmental BPA exposure was achieved through oral administration of 100 or 250  $\mu$ g BPA/kg body weight to hosts for 2 weeks after grafting, producing free BPA levels of 0.39 and 1.35 ng/mL serum, respectively. Carcinogenesis was driven by testosterone plus E<sub>2</sub> treatment for 2 to 4 months to model rising E<sub>2</sub> levels in aging men. The incidence of high-grade prostate intraepithelial neoplasia and adenocarcinoma markedly increased from 13% in oil-fed controls to 33% to 36% in grafts exposed in vivo to BPA ( $P < .05$ ). Continuous developmental BPA exposure through in vitro (200 nM) plus in vivo (250  $\mu$ g/kg body weight) treatments increased high-grade prostate intraepithelial neoplasia/cancer incidence to 45% ( $P < .01$ ). Together, the present findings demonstrate that human prostate stem-progenitor cells are direct BPA targets and that developmental exposure to BPA at low doses increases hormone-dependent cancer risk in the human prostate epithelium. (*Endocrinology* 155: 805–817, 2014)

Prostate cancer is the most common noncutaneous cancer and the second leading cause of cancer-related mortality in men in the United States (1). Despite extensive research, the etiology of prostate cancer remains elusive. Further understanding of factors that contribute to this high disease rate are essential for implementing effective

tumor prevention and therapeutic strategies. It is well recognized that adult androgens and estrogens play fundamental roles in initiation, promotion, and progression of prostate cancer (2). There is also compelling evidence that the developmental hormonal milieu may be linked to the predisposition of this gland to prostate cancer in adult

ISSN Print 0013-7227 ISSN Online 1945-7170

Printed in U.S.A.

Copyright © 2014 by the Endocrine Society

Received October 17, 2013. Accepted December 18, 2013.

First Published Online January 7, 2014

For News & Views see page 656

Abbreviations: APC, allophycocyanin; BPA, bisphenol A; BPA-G, glucuronidated BPA; BW, body weight; 2-D, 2-dimensional; 3-D, 3-dimensional; E<sub>2</sub>, estradiol-17 $\beta$ ; EDC, estrogen-disrupting chemical; ER, estrogen receptor; ERE, estrogen response element; EtOH, ethanol; FACS, fluorescence-activated cell sorting; LOD, limits of detection; p, phosphorylated; PIN, prostatic intraepithelial neoplasia; PrEC, primary human prostate epithelial cell; PSA, prostate-specific antigen; SQM, squamous metaplasia; SRM, selected reaction monitoring; T+E, testosterone and estradiol-17 $\beta$ ; UGM, urogenital sinus mesenchyme.

men. Although in utero prostate morphogenesis is driven by fetal androgens (3), maternal and fetal estrogens also modulate development through estrogen receptors (ERs)  $\alpha$  and  $\beta$  expressed in the human fetal prostate (4). Importantly, multiple epidemiology studies link elevated estrogen levels during pregnancy to increased risk of prostate cancer in male offspring (5–9). This is supported by extensive laboratory-based research using rodent models, which has shown that inappropriate estradiol exposure during development in terms of levels and timing can reprogram the developing prostate gland and increase its susceptibility for prostate cancer during aging (10–13). Together, these findings have led to the hypothesis that an altered steroid balance during prostate gland formation, with a shift favoring estrogen dominance, may predispose the newborn male to prostatic disease including carcinoma later in life.

There is rising concern that exposures to endocrine-disrupting chemicals (EDCs) in the environment during sensitive developmental stages may likewise increase susceptibility to prostate cancer in the human population. One ubiquitous EDC with proven estrogenic activity is bisphenol A (BPA), a high-production chemical found in thousands of consumer products including polycarbonate bottles, epoxy resins, carbonless paper receipts, and dental sealants (14, 15). Importantly, BPA monomers have been shown to leach into food and beverages as well as absorb across the skin (15, 16). In a study of 2500 US adults, 93% had detectable urine BPA, indicating that humans are chronically exposed to this compound during routine daily activity (17). Although adults have a high capacity to rapidly metabolize and excrete BPA, the fetus and infant have lower hepatic expression of its metabolizing enzyme, UGT2B, and thus are at greater exposure risk to unconjugated (bioactive) BPA than adults (18). Although levels of unconjugated or free BPA in adult human serum are typically low (undetectable to  $\sim 0.5$  ng/mL), higher levels have been reported in amniotic fluid, fetal circulation, and neonates (19–22). Thus, there is considerable potential for BPA to act as an environmental estrogen in the developing prostate.

To address this possibility, our laboratory used a rat model and demonstrated that similar to estradiol, a brief, early-life exposure to low-dose BPA markedly increased the incidence of later-life, estrogen-mediated prostate carcinogenesis (23, 24). These findings suggest that developmental BPA exposure can sensitize the prostate to adult estrogenic exposures, thus priming their carcinogenic susceptibility to the relative rise in estrogen levels that occur in aging men. Mechanisms for these life-spanning effects were shown to include permanent epigenetic modifications (23, 25) and reprogrammed prostate stem cells (26,

27), which are both retained throughout life. A major issue that remains to be resolved is whether this reprogramming process may occur in the human prostate gland and whether early-life BPA exposures may increase prostate cancer risk in men as they age, as predicted by animal models. However, direct methods for examining developmental BPA exposures and later life prostate cancer incidence in humans is a particular challenge due to the long latency period between fetal development and age of prostate cancer onset (50–60 years).

Recently, our laboratory established a novel model for in vivo development of humanized prostate-like tissues by using epithelial stem-progenitor cells cultured from prostate glands of young, disease-free men (28). Remarkably, we found that the prostate stem-progenitor cells express ERs ( $\alpha$  and  $\beta$ ) and GPR30 and exhibit a proliferative response to 1 nM estradiol-17 $\beta$  ( $E_2$ ), implicating them as direct estrogenic targets. When mixed with embryonic rat urogenital sinus mesenchyme (UGM) and grafted under the kidney capsule of nude mice, these progenitor cells formed normal human prostate epithelium that produce prostate-specific antigen (PSA) within the prostate-like tissues by 1 month of age. Treatment of the host mice bearing the humanized prostate-like structures with testosterone and estradiol-17 $\beta$  (T+E) induced prostate epithelial pathology over a 1- to 4-month period, progressing from hyperplasia to prostatic intraepithelial neoplasia (PIN) and adenocarcinoma at a relatively low incidence (28). Together, these findings provided the first direct evidence that human prostate stem and progenitor cells are direct estrogen targets and that estrogen, in an androgen-supported milieu, is a carcinogen for human prostate epithelium.

In this context, the present study first assessed whether BPA over a range of doses has similar estrogen-like effects on normal human prostate stem-progenitor cells in terms of self-renewal capacity, differentiation, and signaling activity. Next, our in vivo humanized prostate system was used to determine whether developmental stage BPA exposures could modulate the incidence of estrogen-mediated carcinogenesis in the human prostate epithelium as the tissues aged. Importantly, circulating levels of free (bioactive) and glucuronidated BPA (BPA-G) in the host mice after oral exposures were directly measured using an ultra-high-performance liquid chromatography tandem mass spectrometry (UHPLC-MS-MS) system and found to be relevant to human exposures. Our findings reveal that BPA mimics estradiol effects on human prostate stem-progenitor cell self-renewal capacity and that brief exposure of the human prostate epithelium to low-dose BPA during a developmental stage significantly increases the incidence of estrogen-mediated PIN and prostate cancer.

## Materials and Methods

### Cell and prostatesphere cultures

Primary human prostate epithelial cells (PrECs) were obtained from young (19–21 years of age) disease-free organ donors (Lonza) and cultured in prostate epithelial cell growth medium (PrEGM; Lonza) on fibronectin-coated flasks. PrEC from 4 donors were used, and all exhibited similar growth and hormone-responsive behaviors. Prostatespheres were cultured from PrECs as described previously (28) and confirmed as clonally derived spheroids of stem-progenitor cells (Supplemental Figure 1 published on The Endocrine Society's Journals Online web site at <http://end.endojournals.org>). In brief,  $1 \times 10^5$  PrECs were resuspended in 1:1 Matrigel (BD Biosciences)/PrEGM with 1 mL of PrEGM and cultured at 37°C in 5% CO<sub>2</sub>. Prostatespheres were cultured in the absence or presence of 1 nM to 1 μM E<sub>2</sub> (Sigma-Aldrich) or 0.1 nM to 1 μM BPA with medium replenished every 48 hours. Crystalline BPA was provided by the National Toxicology Program (NIEHS), dissolved in 100% ethanol (EtOH) with a final EtOH concentration at 0.1%. Prostatesphere number and size at day 7 were assessed using an automated digital image processing algorithm (see Supplemental Methods and Supplemental Figure 2).

### Flow cytometry

Analysis of the stem-enriched population in day 7 prostatespheres after E<sub>2</sub> exposure was performed by fluorescence-activated cell sorting (FACS) using the CD49f and Trop2 antibody method (29, 30). In brief, prostatespheres were dispersed into single cells, which were stained with anti-human/mouse CD49f allophycocyanin (APC) and anti-human Trop2 Alexa Fluor 488 (eBioscience) antibodies. Dead cells were gated by propidium iodide staining. Mouse IgG2a K isotype control Alexa Fluor 488 and Rat IgG2a K isotype control APC (eBioscience) antibodies were used as negative controls. Cells were sorted using the CyAn ADP analyzer (Beckman Coulter), and events were analyzed and plotted based on CD49f and Trop2 staining intensity by the Summit Software v4.3 (Beckman Coulter). Subpopulations of fractionated cells were further delineated using the Summit Software polygone tool.

### Stem-like cell Hoechst exclusion assay

A Hoechst dye exclusion assay (31, 32) was used to quantitate the fraction of stem-like cells in primary PrEC cultures after exposure to 1 to 100 nM E<sub>2</sub> or 10 nM to 1 μM BPA for 72 hours. PrECs were preincubated for 10 minutes with or without 50 μM verapamil hydrochloride (Sigma-Aldrich), which inhibits ABCG2 transporter protein expressed at high levels in stem cells, blocking their Hoechst exclusion ability. Cells were next incubated in 0.5 μg/mL Hoechst 33342 (Sigma-Aldrich) in Hanks' balance salt solution, 10% fetal bovine serum, 1% D-glucose, and 20 mM HEPES for 30 minutes at 37°C, washed in PBS, and incubated with 1 μg/mL propidium iodide for dead cell exclusion. Hoechst-stained cells were separated by single-channel FACS (CyAn ADP analyzer). All results were confirmed by side-population double-channel FACS analysis (MoFlo XDP analyzer; Beckman Coulter) using 5 μg/mL Hoechst dye (32). The percentage of prostate stem-like cells were calculated as the difference in Hoechst excluding cells incubated without or with verapamil.

### Quantitative real-time RT-PCR

Total RNA was isolated from prostatespheres using RNeasy Mini Kit (QIAGEN), and cDNAs were synthesized using iScript Reverse Transcription Supermix (Bio-Rad). PCR reactions in SsoAdvanced SYBR Green Supermix (Bio-Rad) were performed using a CFX96 Real-Time System (Bio-Rad). Primer sequences for prostate genes are provided in Supplemental Table 1. The cycling conditions were 95°C for 5 minutes, followed by 40 cycles of 95°C for 15 seconds and 60°C for 1 minute. Data were analyzed by the  $-\Delta\Delta C_t$  method, and individual mRNA levels were normalized to the housekeeping gene *RPL13*.

### Estrogen and BPA signaling pathway analysis

To assess rapid, membrane-initiated signaling actions of E<sub>2</sub> and BPA, day 7 prostatespheres (20 000/treatment) were isolated with dispase, resuspended in PrEGM, and exposed to 10 nM E<sub>2</sub> or 10 nM BPA for 0, 15, 30, or 60 minutes or 6 hours at 37°C. Prostatespheres were Dounce homogenized and lysed in cell lysis buffer (Cell Signaling) for 10 minutes at 4°C as described previously (33). Lysates were centrifuged (15 000 rpm) and 30 μg of supernatant protein was separated via 10% SDS-PAGE gels, transferred to polyvinylidene difluoride membranes and immunoblotted. Primary antibodies against phosphorylated (p)-Akt (S473), Akt, p-Erk (Thy202/Tyr204), and Erk (Cell Signaling) and horseradish peroxidase-conjugated secondary antibody were used. Proteins were visualized with Pierce ECL Plus and scanned using ImageQuant (GE Healthcare).

To assess evidence of E<sub>2</sub> or BPA genomic signaling through an estrogen response element (ERE), prostatespheres were cultured for 5 days, isolated from Matrigel with dispase, plated at 200 prostatespheres/well and incubated in PrEGM for 16 hours. Spheres were cotransfected with a firefly luciferase reporter construct, ERE2-tk-luc (34), and *Renilla* luciferase reporter as internal control using lipofectamine for 6 hours. Transfected prostatespheres were treated with vehicle, 10 nM E<sub>2</sub>, or 10 nM to 1 μM BPA for 16 hours, and luciferase activity was measured using a Dual-Luciferase Reporter Assay System (Promega). The ratio of firefly luciferase activity and *Renilla* activity was used to analyze ERE activation by E<sub>2</sub> or BPA over vehicle control. pGL basic vector and pGL3 control vectors were used as negative and positive controls, respectively.

### Animals and formation of humanized prostate-like tissues

Animals were handled according to the Guide for the Care and Use of Laboratory Animals, and studies were approved by the institutional animal care committee. Timed pregnant female Sprague-Dawley Hsd:SD rats were purchased from Harlan, and fetal pups were collected on gestation day 17 for UGM recovery. Male nude mice were purchased from Harlan at 4 to 6 weeks of age and acclimated to BPA-controlled conditions before their use as renal graft hosts. Care was taken to avoid all polycarbonate and epoxy resin contact to the animals, sera, and tissue samples. All materials were screened for BPA content using UHPLC-MS-MS and only products with no detectable BPA levels were used. Animals were housed at 21°C, on a 14:10-hour light/dark schedule in polysulfone solid-bottom cages and double-deionized water was supplied from glass bottles. Animals were fed ad libitum a phytoestrogen-reduced diet (Teklad 2018; Harlan). Food lots with <20 pmol of estrogen equivalents/g, measured by

an E-SCREEN assay (35) were used. In vivo formation of humanized prostate-like structures was performed using tissue recombination and renal grafting in host mice as described previously (28). In brief, ~3000 human prostate epithelial stem-progenitor cells from dispersed day 7 prostaspheres were mixed with rat UGM in Matrigel and grafted under the renal capsule of host adult male nude mice. Mature chimeric prostate-like structures with normal histology formed by 1 month. PSA immunostaining was used to confirm the human origin of the prostate epithelium.

### Developmental in vivo BPA exposure and hormonal carcinogenesis

To recapitulate developmental BPA exposure for the human prostate epithelium, host mice were fed BPA (in 30  $\mu$ L of tocopherol-stripped corn oil, 1% EtOH) daily by mouth for 2 weeks after renal grafting when stem-progenitor cells cytodifferentiate to basal and luminal cells and form glandular structures. Because adult host mice have greater BPA-metabolizing capacity than the fetus (36), preliminary studies were conducted using 50 to 500  $\mu$ g BPA/kg body weight (BW) to identify oral doses that produce internal free BPA levels comparable to levels found in human umbilical cord, fetal serum, and neonatal serum. Four treatment groups were subsequently used: (1) vehicle (n = 38), (2) 100  $\mu$ g BPA/kg BW (n = 36), (3) 250  $\mu$ g BPA/kg BW (n = 27), and (4) 200 nM BPA during in vitro prostasphere culture plus 250  $\mu$ g BPA/kg BW (n = 42). The latter group models BPA exposure from the stem cell stage through prostate morphogenesis in vivo. Tail vein blood was collected from host mice 20 to 30 minutes after feeding on exposure day 7 for quantitation of internal BPA levels. After 1 month, hormonal carcinogenesis was initiated through subcutaneous T+E pellets (25 mg of T and 2.5 mg E<sub>2</sub>), which models rising E<sub>2</sub> levels in aging men and promotes progressive carcinogenesis over 4 months (28). Host mice were euthanized at 2 and 4 months, and the renal grafts were collected.

### Histology and immunohistochemistry

Grafted tissues were fixed in methacarn, dehydrated, and embedded. Serial sections were stained with hematoxylin and eosin, coded, and examined by 2 board-certified pathologists blinded to treatment. Tissues were classified for human prostate pathology according to criteria established by the Armed Forces Institute of Pathology and categorized as normal, squamous metaplasia (SQM), epithelial hyperplasia, high-grade (HG)-PIN, and adenocarcinoma. Although multiple benign (SQM and hyperplasia) and malignant (HG-PIN and cancer) lesions coexisted in several grafts, the malignancy incidence was ranked based on the most severe lesion present. Immunohistochemical analysis was performed for confirmation of human prostate epithelial lesions using PSA, p63, CK14, and CK 8/18 as described previously (28).

### Bisphenol A quantitation

HPLC-grade solvents (acetonitrile, methanol, and water) were purchased from Burdick & Jackson (Honeywell) and were determined to be free of BPA contamination. BPA and [*ring*-<sup>13</sup>C<sub>12</sub>]-BPA-G were purchased from Sigma-Aldrich. Bisphenol A mono- $\beta$ -D-glucuronide (BPA-G) was obtained from the Midwest Research Institute. [*d*<sub>6</sub>]-BPA was purchased from Cambridge Isotope Laboratories.

Stock solutions of BPA and BPA-G were prepared in methanol at a final concentration of 1 mg/mL and stored in amber glass

vials. Working standards were made by serial dilution from stock solutions. Calibration standards were prepared by mixing 1  $\mu$ L of each working standard with 24  $\mu$ L of blank mouse serum and vortex mixing. Each unknown serum sample (25  $\mu$ L) or calibration standard (25  $\mu$ L) was mixed with 100  $\mu$ L of acetonitrile containing the surrogate standards 5 ng/mL [*d*<sub>6</sub>]-BPA and 5 ng/mL [<sup>13</sup>C<sub>12</sub>]-BPA-G. The mixture was vortexed for 1 minute, centrifuged for 15 minutes at 13 000  $\times$  g at 4°C, and the supernatant was removed and evaporated to dryness. The residue was reconstituted in 25  $\mu$ L of 50% aqueous methanol and a 5- $\mu$ L aliquot was injected onto the UHPLC-MS-MS system for analysis.

Chromatographic separations were carried out using a Shimadzu LCMS-8050 triple quadrupole mass spectrometer equipped with a Shimadzu Nexera UHPLC system. BPA and BPA-G were separated on a Waters Acquity UPLC BEH (2.1  $\times$  50 mm, 1.7  $\mu$ m) C<sub>18</sub> column. A 1.5-minute linear gradient was used from 10% to 100% acetonitrile in water followed by a hold at 100% for 0.3 minute at a flow rate of 0.4 mL/min. The total run time including equilibration was 3.5 minutes. The column oven temperature was 45°C. Negative ion electrospray mass spectrometry with selected reaction monitoring (SRM) was used for the measurement of each analyte. Two SRM transitions (quantifier and qualifier) were monitored for each analyte as follows: BPA *m/z* 227 to 212 and *m/z* 227 to 133; [*d*<sub>6</sub>]-BPA *m/z* 233 to 215 and *m/z* 233 to 113; BPA-G *m/z* 403 to 227 and *m/z* 403 to 113; and [<sup>13</sup>C<sub>12</sub>]-BPA-G *m/z* 415 to 239 and *m/z* 415 to 113. The SRM dwell time was 50 milliseconds per transition. The lower limits of quantitation for BPA and BPA-G were 0.5 and 0.2 ng/mL, respectively, and the lower limits of detection (LOD) for BPA and BPA-G in mouse serum were 0.2 and 0.1 ng/mL, respectively.

### Statistical analysis

For in vitro studies, data were analyzed by a Student *t* test or ANOVA followed by post hoc tests (GraphPad Software Inc). For in vivo studies, power analysis determined an n = 23/group was required for appropriate power; thus, a minimum of 25/group was used in the present studies. Analysis of prostate lesion incidence between groups was performed using the Fisher exact test. Values are expressed as means  $\pm$  SEM, and a value of *P* < .05 was considered significant.

## Results

### Estradiol and BPA stimulate human prostate stem cell self-renewal and progenitor cell amplification

Initial studies had demonstrated that 1 nM E<sub>2</sub> exposure increased prostasphere number and size at day 7, indicative of a stimulation in stem cell self-renewal and progenitor cell proliferation, respectively (28). To determine the dose response to E<sub>2</sub>, prostaspheres were cultured in 1 nM to 1  $\mu$ M E<sub>2</sub> for 7 days. As shown in Figure 1A, the maximal stimulatory effect of E<sub>2</sub> on sphere number and size was observed at 1 nM with higher E<sub>2</sub> doses having no further increase in 40- to 80- $\mu$ m sphere numbers and a decreasing effect observed on spheroids >80  $\mu$ m. Next, prostas-

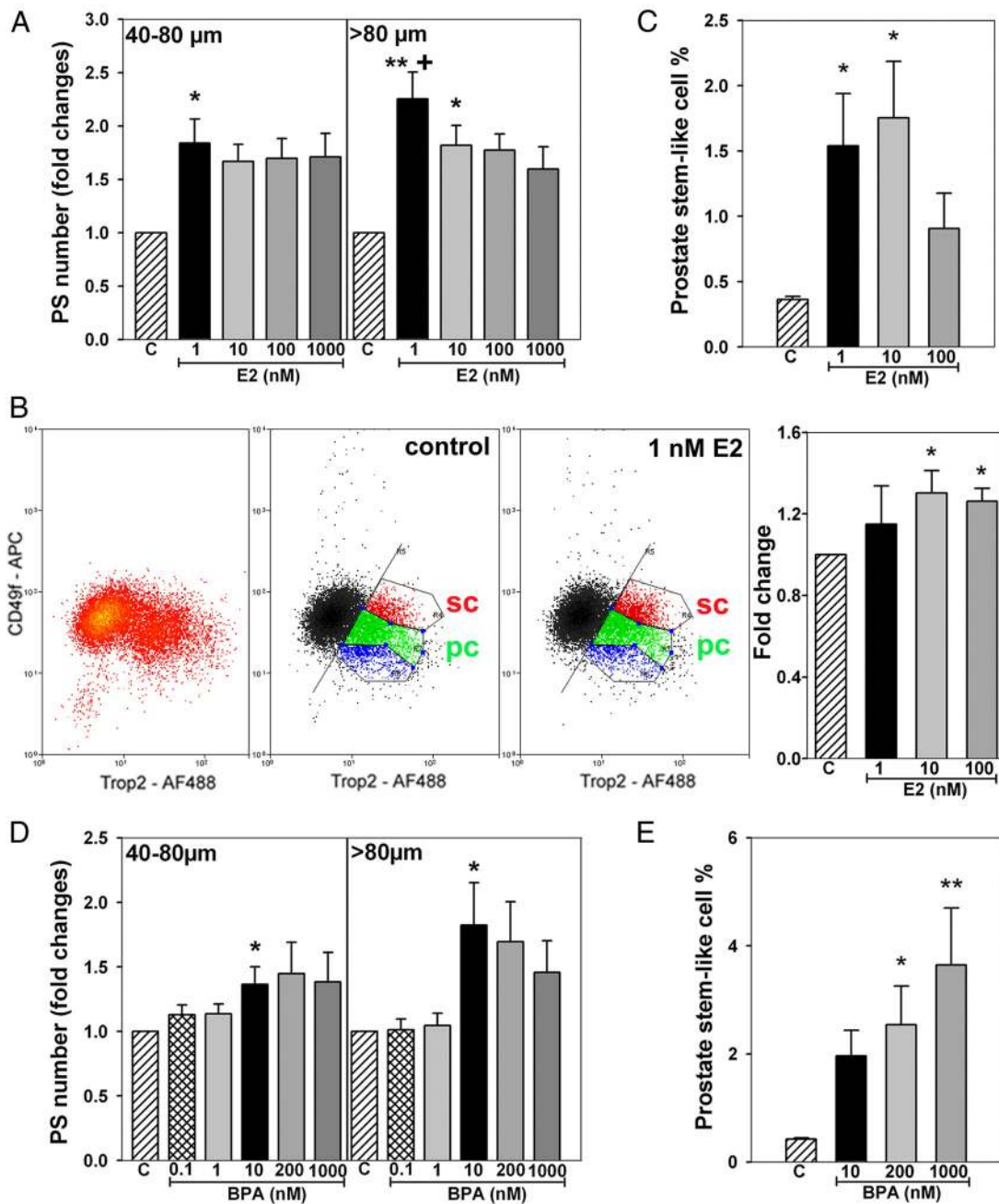


**Figure 1.** Dose-response effects of E<sub>2</sub> and BPA on prostasphere growth and self-renewal of stem-like cells in primary prostate epithelial cell cultures. A, Prostraspheres (PS) were grown for 7 days in a 3-D Matrigel culture in the absence (C) or presence of 1 nM to 1 μM E<sub>2</sub>. Prostrasphere number and size (40–80 μm, >80 μm diameter) were measured by digital imaging (n = 6). \*, P < .05; \*\*, P < .01 vs vehicle control, +, P < .05 vs 1 μM E<sub>2</sub>. B, Prostraspheres cultured for 7 days with vehicle or 1 to 100 nM E<sub>2</sub> were dispersed and FACS sorted using CD49f APC and Trop2 Alexa Fluor 488 (AF488) antibodies. Summit software polygonal analysis of Trop2<sup>+</sup> cells identified a Trop2<sup>+</sup>/CD49f<sup>Med</sup> cell subpopulation (red) designated as stem-like cells (sc) and a Trop2<sup>+</sup>/CD49f<sup>Med</sup> subpopulation (green), classified as early-stage progenitor cells (pc). Representative images of flow cytometry scatter plots are shown without and with polygonal frames for spheres treated with control vehicle or 1 nM E<sub>2</sub>. Exposure to 1 to 100 nM E<sub>2</sub> increased the percentages of TROP2<sup>+</sup>/CD49f<sup>Hi</sup> stem-like cells in the day 7 prostraspheres. \*, P < .05 vs control (n = 3). C, Parental 2-D PrECs (n = 6) were treated with 1 to 100 nM E<sub>2</sub> for 72 hours, and the percentage of prostate stem-like cells was evaluated by Hoechst dye exclusion–based flow cytometry; 1 to 10 nM E<sub>2</sub> increased the stem-like cell population. \*, P < .05 vs control (n = 6). D, Prostraspheres were cultured for 7 days in the absence (C) or presence of 0.1 nM to 1 μM BPA, and prostrasphere number and size were digitally analyzed. A stimulatory effect was first noted at 10 nM BPA. \*, P < .05 vs control (n = 5). E, Parental 2-D PrECs were treated with 10, 200, or 1000 nM BPA for 72 hours, and the Hoechst dye exclusion assay with FACS was used to determine the percentage of stem-like cells present. Treatment with increasing BPA doses augmented the stem-like cell fraction, suggesting stimulation of stem cell self-renewal. \*, P < .05; \*\*, P < .01 vs vehicle control (C) (n = 6).

pheres cultured for 7 days in 1 to 100 nM E<sub>2</sub> or vehicle were dispersed, and FACS was used for Trop2<sup>+</sup>/CD49f<sup>Hi</sup> cells (Figure 1B). The mixed stem and progenitor cells were CD49f<sup>+</sup>, whereas staining for Trop2<sup>+</sup> delineated a distinct subset of cells outside of the main population. Polygonal analysis of the Trop2<sup>+</sup> population demarcated distinct CD49f<sup>+</sup> subpopulations with Trop2<sup>+</sup>/CD49f<sup>Hi</sup> designated as stem-like cells and Trop2<sup>+</sup>/CD49f<sup>Med</sup> stained cells classified as early stage progenitor cells. Importantly, exposure to E<sub>2</sub> increased the proportion of Trop2<sup>+</sup>/CD49f<sup>Hi</sup> stem-like cells in day 7 prostaspheres in a dose-dependent manner with the maximal effects observed at 10 nM E<sub>2</sub> (Figure 1B). For further confirmation, a Hoechst exclusion assay was used to quantitate the stem-like cell side population in parental primary cultures after E<sub>2</sub> exposure for 72 hours. Similar to the prostasphere assay, 1 to 10 nM E<sub>2</sub>, but not 100 nM, significantly increased the percentage of stem-like cells in primary cultures, in-

dicating a stimulation of their self-renewal capacity (Figure 1C). Collectively, these findings show that estrogen stimulates human prostate epithelial stem cell self-renewal and progenitor cell amplification (prostasphere size), with the greatest effects observed at lower E<sub>2</sub> doses.

Next, 3-dimensional (3-D) prostasphere and 2-dimensional (2-D) primary prostate epithelial cell cultures were exposed to BPA over a 0.1 nM to 1 μM dose range. Similar to E<sub>2</sub>, BPA increased prostasphere number and size with significant and maximal effects observed at 10 nM BPA (Figure 1D). Although higher BPA levels also increased 40- to 80-μm sphere numbers, the stimulatory effect was reduced on spheres >80 μm in size compared with 10 nM BPA. Interestingly, FACS analysis of Hoechst-excluding cells in the primary cell cultures showed a marked dose-dependent increase in prostate stem-like cells after 72 hours of BPA exposure, with maximal effects observed at 1 μM BPA (Figure 1E). Taken together, these results provide

strong evidence that, similar to E<sub>2</sub>, BPA increases stem cell self-renewal and progenitor amplification in normal human prostate epithelial cells. Further, because the dose-response patterns for E<sub>2</sub> and BPA exhibit notable differences, the findings also suggest some nonoverlapping actions for the 2 chemicals.

### Estradiol and BPA enhance expression of prostasphere stemness genes

The expression of genes associated with stemness and epithelial cell differentiation was evaluated in day 7 prostaspheres cultured in 1 nM E<sub>2</sub>, 10 or 200 nM BPA. Exposure to 1 nM E<sub>2</sub> markedly increased expression of *CD49f*, *TROP2*, *ABCG2*, *FOXM1*, *BMI1*, *TBX3*, *SOX2*, and *NANOG* (Figure 2, A and B). In a similar manner, BPA exposure increased expression of some, but not all, stemness genes with a significant increase in *TBX3* and *NANOG* in response to 200 nM and a similar trend at 10 nM BPA (Figure 2B). Expression of epithelial cell differentiation genes *NKX3.1*, *HOXB13*, and *CK18* was at the lower limit of detection in day 7 prostaspheres, and this was not influenced by E<sub>2</sub> or BPA exposure (Figure 2C). Taken to-

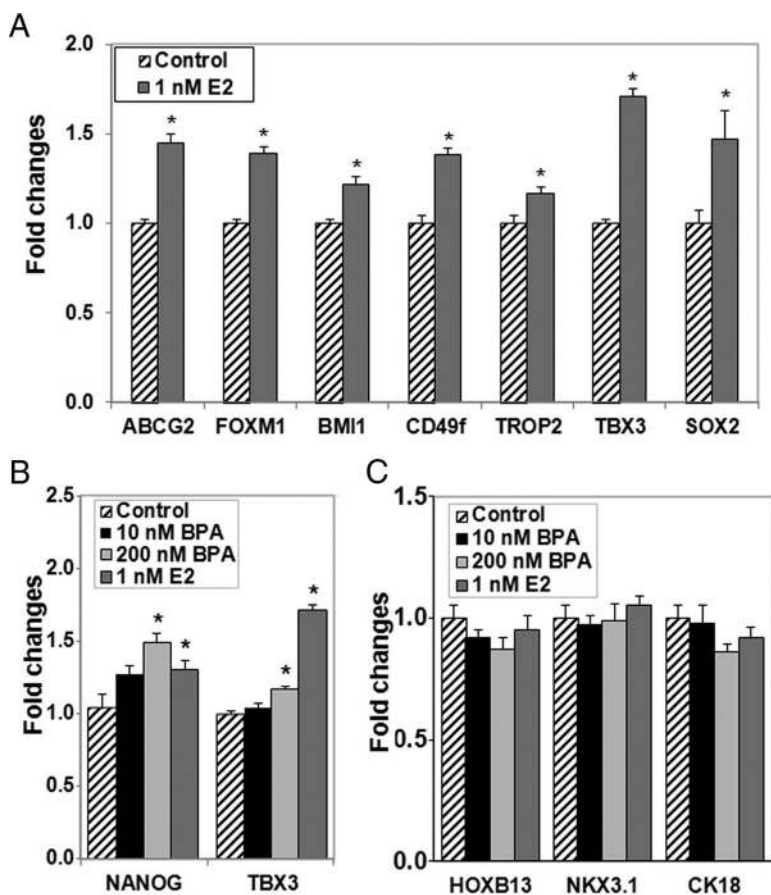


**Figure 2.** Estradiol and BPA augment expression of prostasphere stemness genes and do not alter genes associated with cell differentiation. Prostaspheres were grown for 7 days in a 3-D Matrigel culture in the absence or presence of 1 nM E<sub>2</sub>, 10 or 200 nM BPA. A, 1 nM E<sub>2</sub> treatment significantly increased gene expression of all stem cell genes examined, including *ABCG2*, *FOXM1*, *BMI1*, *CD49f*, *TROP2*, *TBX3*, and *SOX2*. B, Similar to 1 nM E<sub>2</sub>, 200 nM BPA significantly increased *NANOG* and *TBX3* expression. C, E<sub>2</sub> and BPA exposures did not alter *HOXB13*, *NKX3.1*, or *CK18* expression, indicating lack of influence on entry into the differentiated luminal cell lineage. \*, *P* < .05 vs vehicle control (*n* = 4–6 assays from separate donor cultures).

gether, these findings provide further support that E<sub>2</sub> and BPA maintain the stem-like state within the normal prostate epithelial cell population and again highlight the fact that subtle differential responses may exist between the separate chemicals.

### Estradiol and BPA have equimolar activational capacity for ER rapid signaling pathways but differential genomic ERE capacity in human prostatespheres

Our previous findings demonstrated that normal prostate stem-progenitor cells within the prostatespheres expressed ER $\alpha$  and ER $\beta$ , implicating them as direct targets for E<sub>2</sub> and BPA action (28). In the present study, we sought to ascertain whether E<sub>2</sub> and BPA effects were mediated through membrane-initiated ER signaling pathways and/or through classic nuclear genomic signaling mechanisms. To assess rapid signaling at the membrane, day 7 prostatespheres were briefly exposed to 10 nM E<sub>2</sub> or BPA for 15, 30, or 60 minutes or 6 hours and assessed for p-Akt and p-Erk, well established downstream targets of membrane-associated ERs (37). Both 10 nM BPA and E<sub>2</sub> markedly increased p-Akt levels within 15 minutes with sustained levels for 60 minutes and reduction to baseline levels by 6 hours (Figure 3A). A nearly identical pattern was observed for Erk phosphorylation (Figure 3B). Importantly, BPA and E<sub>2</sub> had equimolar capacity for activa-

tion of these rapid signaling pathways in human prostatespheres, thus identifying a dynamic and robust signaling pathway initiated by low-dose BPA exposure in prostate stem-progenitor cells.

To identify whether classic genomic signaling (ie, nuclear receptor-based transcription) is operative in human prostate progenitor cells, an ERE-luciferase reporter was transiently transfected into day 5 prostatesphere cells followed by E<sub>2</sub> or BPA exposures. As seen in Figure 3C, 10 nM E<sub>2</sub> stimulated tk-luciferase activity above that of vehicle-treated cells at levels equivalent to those of the positive control, providing direct evidence that genomic ER signaling pathways are intact in the early progenitor cells of the human prostate. Similar E<sub>2</sub> responses were seen with a pS2-luciferase reporter (data not shown). In contrast, BPA at doses up to 1  $\mu$ M did not elicit ERE-based responses with the ERE-tk reporter (Figure 3C). Although genomic actions of BPA through EREs could not be confirmed in the present study, this activity has not been excluded because it remains possible that BPA may activate genomic ER signaling on natural promoters or over a different time frame than examined herein. Taken together, these findings indicate that both rapid membrane-initiated estrogen action and genomic ER signaling pathways are operative in human prostate progenitor cells. Equimolar rapid actions for BPA and E<sub>2</sub> through membrane-initiated

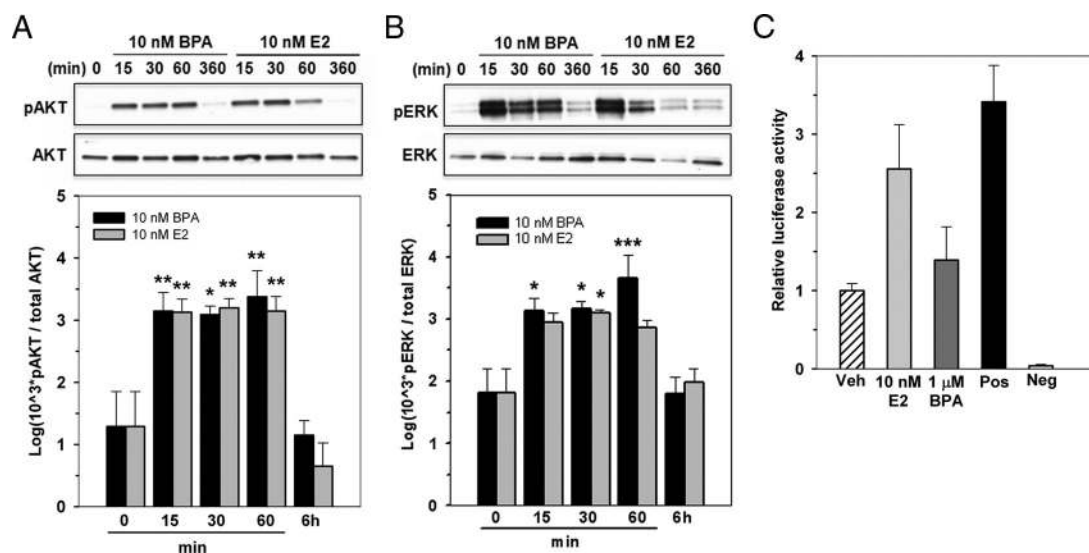


**Figure 3.** Estradiol and BPA have equimolar activational capacities for ER rapid signaling pathways but differential genomic ERE capacity in human prostatespheres. A and B, Day 7 prostatespheres grown in the absence or presence of 10 nM BPA or E<sub>2</sub> (n = 4) for 15, 30, or 60 minutes or 6 hours were assessed for p-Akt/total Akt (A) and p-Erk/total Erk (B) by Western blot assay. Representative blots (top) and graphic representations of densitometry analysis from 4 separate cultures (bottom) are shown. Both 10 nM E<sub>2</sub> and 10 nM BPA markedly increased Akt phosphorylation at 15, 30, and 60 minutes with a return to baseline activity by 6 hours (A). \*, P < .05; \*\*, P < .01 vs vehicle. A similar temporal profile was observed for ERK phosphorylation (B). \*, P < .05; \*\*\*, P < .001 vs vehicle. C, Genomic ERE signaling activity in day 7 prostatespheres was evaluated using an ERE-tk-Luc reporter assay (see *Materials and Methods*). Day 6 prostatespheres pretransfected with the luciferase ERE-tk reporter and a *Renilla*-luciferase control construct were treated with 10 nM E<sub>2</sub> or 1  $\mu$ M BPA for 16 hours, and ERE reporter activity was measured by a Dual-Luciferase Reporter Assay System. E<sub>2</sub> at 10 nM increased tk-luciferase activity ~2.5-fold compared with the vehicle (Veh)-treated cells (n = 3), similar to activity seen in the positive control vector. Treatment with 1  $\mu$ M BPA did not increase luciferase activity above that for vehicle treatment.

signaling provide a mechanistic framework for similar stimulatory actions on stem-progenitor cell numbers in the prostate epithelial cell population. Further, differential genomic-based signaling activities may be responsible for the differential dose responses and stimulation of stemness gene transcription for E<sub>2</sub> and BPA noted in the present studies.

### Developmental-stage, low-dose BPA exposure increases estrogen-driven carcinogenesis of human prostate epithelium

Next, the *in vivo* renal graft model of chimeric human-rat prostate tissues (28) was used to test whether developmental exposure to environmentally relevant levels of BPA would influence the susceptibility of the human prostate epithelium to hormone-driven carcinogenesis, as shown previously in the rat prostate gland (23, 38). Murine hosts were given daily oral exposure to BPA for 2 weeks after renal grafting, and serum samples collected 20 to 30 minutes after feeding were used to quantitate the biologically relevant, internal BPA levels. The highly sensitive UHPLC-MS-MS system allowed direct quantitation of both free BPA and BPA-G in 25  $\mu$ L of sera, thus permitting measurement in individual mice from tail vein sampling (Figure 4A). As shown in Figure 4B, all vehicle-treated control mice had undetectable levels (<LOD) of BPA and BPA-G, documenting the lack of contamination in the system. The circulating free BPA levels in mice fed 100 and 250  $\mu$ g of BPA/kg BW were 0.39 and 1.35 ng/mL,

respectively. Levels of BPA-G were  $\sim$ 10 times higher than those of free BPA, indicating that  $\sim$ 10% of oral-exposed BPA was bioavailable 20 to 30 minutes after ingestion. Together, these results document the fact that levels of bioactive BPA in the present study are similar to levels found in human umbilical cord blood and newborns in the general population (22).

When the chimeric prostate grafts reached maturity at 1 month, hormonal carcinogenesis was initiated/promoted through the administration of T+E pellets for 2 to 4 months. As previously observed (28), incidences of progressive malignancy were noted over time with highest HG-PIN and cancer incidence present at 4 months. Examples of HG-PIN and prostate adenocarcinoma as well as benign lesions of hyperplasia and SQM are shown in Figure 5 with PSA immunostaining to confirm their human origin and lack of basal cell staining to confirm carcinoma. Because the renal graft model is limited to 5 to 6 months, the combined HG-PIN and adenocarcinoma incidence was used as a surrogate for malignant prostatic growth, whereas combined hyperplasia and SQM was used to quantify overall benign lesion incidence within the prostatic tissues. As shown in Table 1, prostate grafts from animals treated with vehicle during tissue development plus T+E exposure at maturity had an overall incidence of 26% normal grafts, 74% benign lesions, and 13% malignant lesions (note that malignant lesions always coappeared in grafts containing benign lesions). Developmental exposure to either 100 or 250  $\mu$ g of BPA/kg BW reduced the normal prostate incidence to 11% and 0% ( $P < .01$ ), respectively, augmented the benign lesion incidence to 89% and 100% ( $P < .05$ ), respectively, and increased the incidence of malignant lesions to 36% and 33%, respectively ( $P < .02$ ). With the addition of *in vitro* BPA exposure to prostaspheres for 7 days before *in vivo* BPA exposure (250  $\mu$ g/kg BW), to model continuous BPA exposure throughout development, the incidence of malignant lesions further increased to 45% ( $P < .05$ ). Taken together, the present findings identify for the first time that *in vivo* BPA exposure of the human prostate epithelium to low doses of BPA significantly increases the susceptibility of the human prostate epithelium to hormonal carcinogenesis.

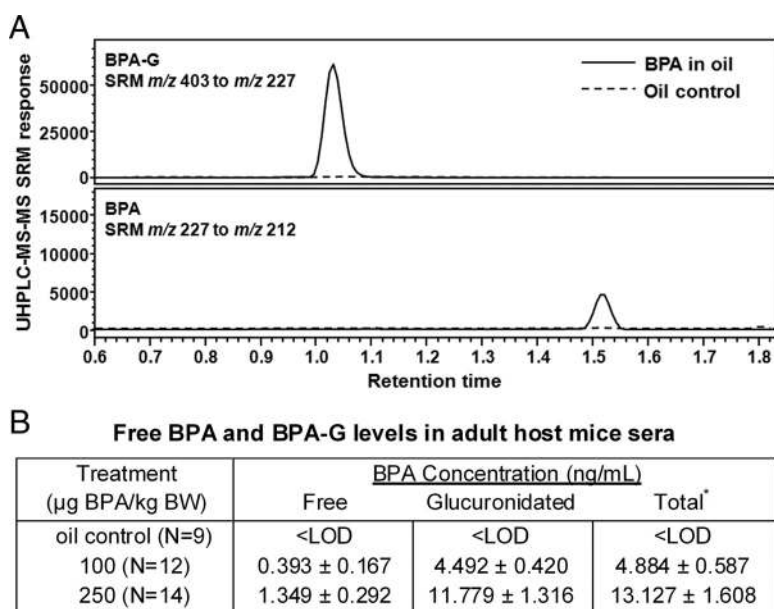


**Figure 4.** BPA and BPA-G quantitation in mouse serum 20 to 30 minutes after oral exposure. A, UHPLC-MS-MS chromatograms showing BPA and BPA-G in mouse serum from animals receiving 250  $\mu$ g of BPA/kg BW in oil (solid line) or oil vehicle as a control (dashed line). B, Levels of free BPA and BPA-G by direct quantitation in sera of individual mice treated with vehicle, 100 or 250  $\mu$ g BPA/kg BW. Sera were collected 20 to 30 minutes after oral exposure on day 7 of daily feeding to adult host mice. \*, Total = free BPA + BPA-G.



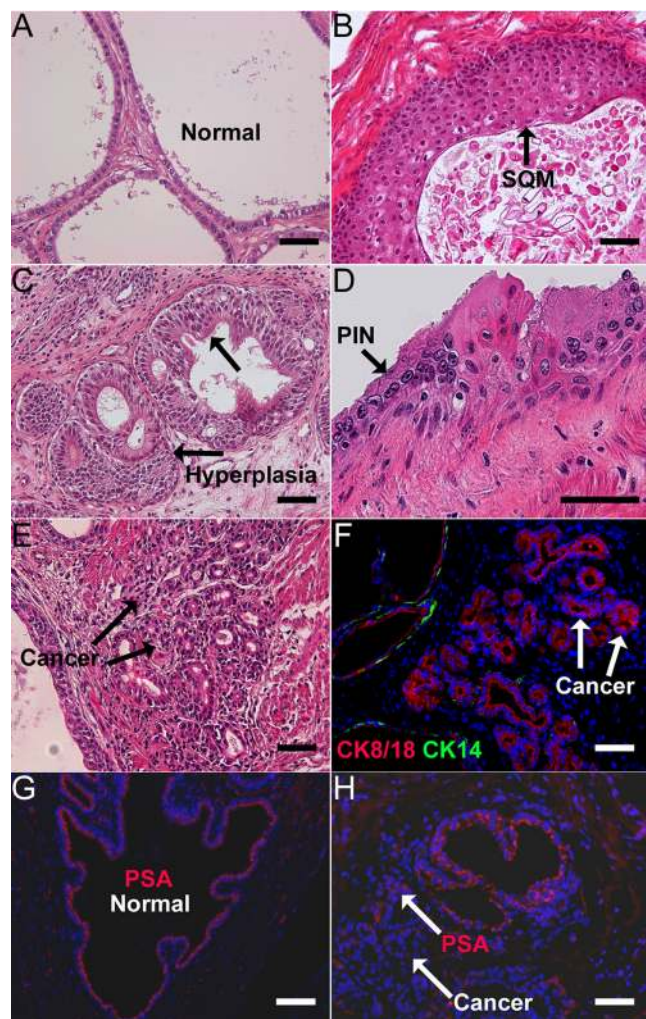


**Figure 5.** Hormonal carcinogenesis in human prostate epithelium of chimeric prostate renal grafts induced by T+E. Hematoxylin and eosin staining and immunofluorescent immunocytochemical analysis was used to classify and confirm prostate pathology in renal graft tissues after 2 to 4 months of T+E treatment to host mice. A, Normal chimeric prostate-like tissue formed from the recombination of human prostatesphere cells with rat UGM after 1 month of growth under the renal capsule of host nude mice. B, SQM was frequently observed in the prostatic grafts after 2 to 4 months of T+E treatment. C, Extensive prostate epithelial hyperplasia with narrowed lumens was observed in most of the tissue grafts after T+E exposure. D, Hormonal carcinogenesis induced by T+E was observed in some chimeric grafts as evidenced by areas of HG-PIN with piling and overlapping epithelial cells, nuclear enlargement, hyperchromasia, and prominent nucleoli. E, Adenocarcinoma of human prostate epithelium in prostatic grafts after T+E exposure. Heterogeneous small glandular-like structures containing epithelial cells with enlarged nuclei and prominent nucleoli within the underlying stromal region. F, Prostate cancer was confirmed using immunofluorescent labeling showing the presence of the luminal epithelial cell marker CK8/18 (red) and the absence of basal cell marker CK14 (green) in the small, glandular-like cancerous regions adjacent to normal ducts (CK14<sup>+</sup>) in the prostatic grafts. G and H, Immunofluorescent labeling for PSA (red) confirms the human identity of the normal prostate epithelium (G) and cancerous areas (H) within the grafted tissues. Scale bars correspond to 50  $\mu$ m.

## Discussion

Increasing evidence has shown that exposure to low levels of BPA can contribute to multiple adverse health outcomes that include behavioral impairment, infertility, metabolic disorders, and increased risk for mammary and prostate cancer (39, 40). The developmental stage has been identified as being particularly sensitive to BPA exposure, a phenomenon attributed to tissue organizational processes and molecular programming that occur early in life (23, 41, 42). In addition, recent findings have shown that stem cells can be reprogrammed by EDCs, which may perpetuate lifelong changes in tissue growth and function (32, 43–45). Although a growing body of work indicates that humans are as susceptible as animals to the adverse effects of BPA, most research on BPA has been derived in animal models (39). In this context, previous work from our laboratory using a rodent model established a direct link between developmental BPA exposure at environmentally relevant doses and increased susceptibility to estrogen-driven carcinogenesis with aging (23–25). At present, there is a compelling need to assess whether the developing human prostate is similarly reprogrammed by low-dose BPA exposures and whether this may influence prostate cancer risk in men as they age.

The current study provides clear evidence that, similar to E<sub>2</sub>, normal human prostate stem and progenitor cells are direct targets for BPA action. Both hormones increased stem-like cell numbers in primary prostate epithelial cultures in a dose-dependent manner and augmented the number and size of 3-D cultured prostaspheres, markers of stem cell self-renewal and progenitor cell proliferation, respectively. Combined with elevated expression of stem cell–related genes including SOX2, NANOG, and TBX3 in the prostaspheres and a lack of effects on differentiation of gene expression, these data indicate that BPA and E<sub>2</sub> have the capacity to amplify the human prostate epithelial stem-progenitor cell populations. This result is supported by a recent study using in vitro differentiation of human embryonic stem cells into mammospheres, which reported that 1 to 100 nM BPA or 1 nM E<sub>2</sub> increased NANOG and OCT4 levels, suggesting an enhancement of stemness within mammary epithelial cells (46). Although BPA failed to promote adipogenesis in murine mesenchymal stem cells, 10 nM BPA was capable of directing preadipocytes to adipocytes, which suggests a stage-specific or lineage-specific effect of BPA on stem and progenitor cell populations (44). In the present study, a dose-response effect was observed with peak stimulatory effects on prostasphere growth observed at 1 nM E<sub>2</sub> and 10 nM BPA and a declining influence noted on sphere size at higher doses, which provides a physiologic and environmentally rele-

**Table 1.** Effects of Developmental BPA Exposure on Pathology Incidence in Human Prostate Epithelium Treated In Vivo With T+E

	Oil	BPA		
		100 $\mu\text{g}/\text{kg}$ BW in vivo	250 $\mu\text{g}/\text{kg}$ BW in vivo	200 nM in vitro, 250 $\mu\text{g}/\text{kg}$ BW in vivo
n	38	36	27	42
Normal, n (%)	10 (26)	4 (11)	0 (0)	4 (10)
<i>P</i> value		.093	.008 <sup>b</sup>	.061
Abnormal: benign				
hyperplasia/SQM, n (%)	28 (74) <sup>c</sup>	32 (89) <sup>c</sup>	27 (100) <sup>c</sup>	38 (90) <sup>c</sup>
<i>P</i> value		.061	.035 <sup>a</sup>	.003 <sup>b</sup>
Abnormal: malignant				
HG-PIN/prostate cancer, n (%)	5 (13) <sup>c</sup>	12 (36) <sup>c</sup>	9 (33) <sup>c</sup>	19 (45) <sup>c</sup>
<i>P</i> value		.016 <sup>a</sup>	.001 <sup>b</sup>	.038 <sup>a</sup>

<sup>a</sup> *P* < .05 vs oil using the Fisher exact test.

<sup>b</sup> *P* < .01 vs oil.

<sup>c</sup> Some specimens contain multiple diagnoses.

vant context to the present data on E<sub>2</sub> and BPA. Although a similar bell-shaped dose response to E<sub>2</sub> levels was found in the stem-like cell population of the parental primary prostate cultures, a linear dose response was noted with rising BPA, reaching maximal effects at 1  $\mu\text{M}$  BPA. These distinct effects are probably driven by activation of different ERs and/or separate downstream signaling pathways by E<sub>2</sub> and BPA in the stem and progenitor cell populations. An alternate possibility is that BPA may engage non-ER pathways in prostate stem cells, as has been shown in other systems including directed differentiated mammospheres (46–48).

Estrogen action is mediated by ER $\alpha$  and ER $\beta$  and may also be initiated by GPR30, all of which are expressed by early-stage human prostate stem-progenitor cells (28). Furthermore, signaling pathways engaged by estrogens through these separate receptors are multiple and complex, including both membrane-initiated signaling and genomic activation via ER transcriptional activity (49, 50). Importantly, the current findings demonstrate that BPA and E<sub>2</sub> at 10 nM concentrations have equimolar activational capabilities in human prostaspheres through membrane-initiated, rapid signaling pathways that include p-Akt and p-Erk. These provide multiple and divergent mechanisms that can be subsequently initiated in prostate stem-progenitor cells by E<sub>2</sub> and BPA through phosphorylation of numerous downstream proteins, leading to altered cellular responses. One recent example was reported in the rat postnatal prostate, in which BPA activated phosphatidylinositol 3-kinase/Akt signaling and rapidly diminished tissue H3K27me3 levels (33), suggesting reduced activity of EZH2, a known downstream action of p-Akt (51). Several studies have previously identified equimolar activational activity between E<sub>2</sub> and BPA

at low doses through rapid signaling pathways in a number of cell types including cardiomyocytes (52), pituitary (53), pancreatic (54), and neural cells (55), and the results herein extend this to a stem-progenitor cell population. The present study also showed differential capacities of E<sub>2</sub> and BPA for classic genomic actions through ER-ERE activation, with 10 nM E<sub>2</sub> showing strong ERE-luciferase induction, whereas no effects were observed on this reporter system by 10 nM to 1  $\mu\text{M}$  BPA. It is important to note, however, that these results do not rule out genomic actions of BPA at natural reporters in prostate stem-progenitor cells but rather emphasize differential transcriptional capacities of E<sub>2</sub> and BPA at reporter constructs. The present findings are consistent with early studies showing that BPA has reduced affinity and activational capacity for nuclear ER-ERE signaling (56). In contrast, a recent report demonstrated ERE-luciferase activation by BPA in Ishikawa cells, HeLa cells, and HepG2 cells cotransfected with ER $\alpha$  or ER $\beta$  at 1 nM to 1  $\mu\text{M}$  doses (57), which suggests that ER expression levels, coactivator availability, and/or cell specificity may contribute to divergent genomic ER responses by BPA. Differential engagement of signaling pathways by E<sub>2</sub> and BPA in the human prostate stem-progenitor cells is the likely basis for nonoverlapping actions of these chemicals in the current work. Studies with the aim of dissecting downstream pathways activated through p-Akt and p-Erk as well the separate roles played by ER $\alpha$  and ER $\beta$  in mediating E<sub>2</sub> and BPA actions on these cell populations are ongoing.

A primary goal of the current studies was to evaluate the potential cancer-promoting actions of developmental exposures to BPA on the human prostate epithelium in vivo. The present findings provide the first evidence that exposure of the developing human prostate epithelium to

BPA at relevant human exposure levels markedly increases the incidence of prostate carcinogenesis in the mature epithelium exposed to elevated estradiol. Taken together, these data contribute to the increasing body of evidence for a link between fetal exposures to EDCs and cancer (58). In vivo BPA exposure during the time of stem-progenitor cell lineage commitment, differentiation, and formation of glandular epithelium significantly boosted the rate of T+E-driven carcinogenesis from 13% in vehicle-exposed hosts to 33% to 36% malignancy. This carcinogenic rate further increased to 45% when developmental BPA exposure was extended to in vitro stem cell cultures, implicating the stem-progenitor cells as the direct BPA targets, a hypothesis supported by the in vitro studies discussed above. That these malignant lesions arose from normal prostate epithelium in the relatively short time frame of 2 to 4 months, compared with decades in humans, is particularly noteworthy and highlights the potent nature of this EDC on augmenting carcinogenic susceptibility. It is important to emphasize that the stem cells in the present study were cultured from disease-free prostates of young organ donors, making it unlikely that the cells had prior initiating events. Thus, BPA exposure is implicated as a potential initiating event in human prostate stem-like cells, one that enables promotion by increasing estrogens later in life, as occurs in aging men (21). This finding is similar to our previous findings in a rat model (23, 24) and provides strong evidence that these earlier rodent data are directly relevant to human disease. The molecular underpinnings of altered prostate memory to estrogenic exposures are probably due to complex reprogramming of the prostate epigenome as shown in our rodent model (23, 25), and studies to identify these specific reprogrammed genes in the human prostate stem-progenitor cells are underway.

The issue of BPA dose levels, route of exposure, pharmacokinetics, potential contamination, and methods of quantitation have raised considerable debate in the recent past (39, 59). Consequently, strict standards must be adhered to when modeling for human disease. To address these concerns, in the present study, we used 2 in vivo oral BPA doses, which accurately model internal dose levels of unconjugated or free BPA observed in human fetal cord blood, fetal serum, and infants, in the adult host mice (16, 60–62). Most recently, a study on midgestational umbilical cord blood in 85 patients using a new analytical approach that permitted direct measurement of free and glucuronidated BPA by LC-MS-MS reported free BPA levels ranging from <LOD (0.05) to 52 ng/mL with a geometric mean of 0.16 ng/mL in human cord serum (22). Of note, they found a subset of midgestation fetuses that had relatively high levels of unconjugated BPA (with levels in

3 fetuses >18 ng/mL) in a system validated as contamination free. Using a similar analytic approach, we herein developed an UHPLC-MS-MS method using labeled BPA and BPA-G standards that permits direct quantitation of free BPA and BPA-G in <25  $\mu$ L of serum. Whereas all vehicle control mice had BPA <LOD, levels of free BPA were 0.39 and 1.35 ng/mL in our 2 dosing groups. This result permits us to conclude that the BPA exposure levels provided to the humanized prostate during a 2-week developmental window are the same as human fetal exposures, making the present findings directly relevant to the daily human experience.

In summary, the present findings demonstrate that the stem-progenitor cells in the normal human prostate gland are direct targets of estrogenic actions and that, similar to  $E_2$ , BPA can activate downstream signaling pathways that lead to increased self-renewal and maintenance of their stem-like nature. We propose that early-life perturbations in estrogen signaling including inappropriate exposure to BPA have the potential to amplify and modify the stem-progenitor cell populations within the human prostate gland and, in so doing, alter the normal homeostatic mechanisms that maintain a growth neutral state throughout life. Importantly, the current results indicate that developmental exposure to BPA, at doses routinely found in humans, significantly increases the cancer risk in human prostate epithelium in response to elevated estrogen levels in an androgen-supported milieu. Because relative estrogen levels rise in aging men, we suggest that humans may be susceptible to BPA-driven prostate disease in a manner similar to that in the rodent models.

## Acknowledgments

We thank Ana Soto (Tufts University) for performing the E-SCREEN assay on food lots used in this study, Jonna Frasor and Benita Katzenellenbogen (University of Illinois) for the ERE-tk-luc, pS2-ERE, and pGL3 reporters, and Lynn Birch for technical and administrative support throughout the studies.

Address all correspondence and requests for reprints to: Gail S. Prins, PhD, Department of Urology, University of Illinois at Chicago, 820 South Wood Street, M/C 955, Chicago, IL 60612. E-mail: gprins@uic.edu.

This work was supported by National Institutes of Health Grants RC2-ES018758, RC2-ES018789, R01-ES-015584, and R01-CA172220.

Disclosure Summary: The authors have nothing to disclose.

## References

1. Siegel R, Naishadham D, Jemal A. Cancer statistics, 2013. *CA Cancer J Clin.* 2013;63:11–30.

2. Bosland MC, Mahmoud AM. Hormones and prostate carcinogenesis: androgens and estrogens. *J Carcinog*. 2011;10:33.
3. Prins GS, Putz O. Molecular signaling pathways that regulate prostate gland development. *Differentiation*. 2008;76:641–659.
4. Adams JY, Leav I, Lau KM, Ho SM, Pflueger SM. Expression of estrogen receptor  $\beta$  in the fetal, neonatal, and prepubertal human prostate. *Prostate*. 2002;52:69–81.
5. Henderson BE, Ross RK, Pike MC. Toward the primary prevention of cancer. *Science*. 1991;254:1131–1138.
6. Ekblom A. Growing evidence that several human cancers may originate in utero. *Semin Cancer Biol*. 1998;8:237–244.
7. Margel D, Fleshner NE. Oral contraceptive use is associated with prostate cancer: an ecological study. *BMJ Open*. 2011;1:e000311.
8. Rahman AA, Lophatananon A, Stewart-Brown S, et al. Hand pattern indicates prostate cancer risk. *Br J Cancer*. 2011;104:175–177.
9. Barker DJ, Osmond C, Thornburg KL, Kajantie E, Eriksson JG. A possible link between the pubertal growth of girls and prostate cancer in their sons. *Am J Hum Biol*. 2012;24:406–410.
10. Santti R, Newbold RR, Mäkelä S, Pylkkänen L, McLachlan JA. Developmental estrogenization and prostatic neoplasia. *Prostate*. 1994;24:67–78.
11. Prins GS, Birch L, Couse JF, Choi I, Katzenellenbogen B, Korach KS. Estrogen imprinting of the developing prostate gland is mediated through stromal estrogen receptor  $\alpha$ : studies with  $\alpha$ ERKO and  $\beta$ ERKO mice. *Cancer Res*. 2001;61:6089–6097.
12. Prins GS, Huang L, Birch L, Pu Y. The role of estrogens in normal and abnormal development of the prostate gland. *Ann NY Acad Sci*. 2006;1089:1–13.
13. Prins GS, Ho SM. Early life estrogens and prostate cancer in an animal model. *J Dev Origins Health Dis*. 2010;1:365–370.
14. Wetherill YB, Akingbemi BT, Kanno J, et al. In vitro molecular mechanisms of bisphenol A action. *Reprod Toxicol*. 2007;24:178–198.
15. Biedermann S, Tschudin P, Grob K. Transfer of bisphenol A from thermal printer paper to the skin. *Anal Bioanal Chem*. 2010;398:571–576.
16. Vandenberg LN, Chahoud I, Heindel JJ, Padmanabhan V, Paumgartten FJ, Schoenfelder G. Urinary, circulating, and tissue biomonitoring studies indicate widespread exposure to bisphenol A. *Environ Health Perspect*. 2010;118:1055–1070.
17. Calafat AM, Ye X, Wong LY, Reidy JA, Needham LL. Exposure of the U.S. population to bisphenol A and 4-tertiary-octylphenol: 2003–2004. *Environ Health Perspect*. 2008;116:39–44.
18. Nahar MS, Liao C, Kannan K, Dolinoy DC. Fetal liver bisphenol A concentrations and biotransformation gene expression reveal variable exposure and altered capacity for metabolism in humans. *J Biochem Mol Toxicol*. 2013;27:116–123.
19. Vandenberg LN, Hauser R, Marcus M, Olea N, Welshons WV. Human exposure to bisphenol A (BPA). *Reprod Toxicol*. 2007;24:139–177.
20. Padmanabhan V, Siefert K, Ransom S, et al. Maternal bisphenol-A levels at delivery: a looming problem? *J Perinatol*. 2008;28:258–263.
21. Vandenberg LN, Chahoud I, Heindel JJ, Padmanabhan V, Paumgartten FJ, Schoenfelder G. Urinary, circulating, and tissue biomonitoring studies indicate widespread exposure to bisphenol A. *Cien Saude Colet*. 2012;17:407–434.
22. Gerona RR, Woodruff TJ, Dickenson CA, et al. Bisphenol-A (BPA), BPA glucuronide, and BPA sulfate in midgestation umbilical cord serum in a northern and central California population. *Environ Sci Technol*. 2013;47:12477–12485.
23. Ho SM, Tang WY, Belmonte de Frausto J, Prins GS. Developmental exposure to estradiol and bisphenol A increases susceptibility to prostate carcinogenesis and epigenetically regulates phosphodiesterase type 4 variant 4. *Cancer Res*. 2006;66:5624–5632.
24. Prins GS, Ye SH, Birch L, Ho SM, Kannan K. Serum bisphenol A pharmacokinetics and prostate neoplastic responses following oral and subcutaneous exposures in neonatal Sprague-Dawley rats. *Reprod Toxicol*. 2011;31:1–9.
25. Tang WY, Morey LM, Cheung YY, Birch L, Prins GS, Ho SM. Neonatal exposure to estradiol/bisphenol A alters promoter methylation and expression of Nsbp1 and Hpcal1 genes and transcriptional programs of Dnmt3a/b and Mbd2/4 in the rat prostate gland throughout life. *Endocrinology*. 2012;153:42–55.
26. Prins GS. Developmental estrogenization of the prostate gland. In: Naz RK, ed. *Prostate: Basic and Clinical Aspects*. Boca Raton, FL: CRC Press; 1997:247–265.
27. Habermann H, Chang WY, Birch L, Mehta P, Prins GS. Developmental exposure to estrogens alters epithelial cell adhesion and gap junction proteins in the adult rat prostate. *Endocrinology*. 2001;142:359–369.
28. Hu WY, Shi GB, Lam HM, et al. Estrogen-initiated transformation of prostate epithelium derived from normal human prostate stem/progenitor cells. *Endocrinology*. 2011;152:2150–2163.
29. Goldstein AS, Lawson DA, Cheng D, Sun W, Garraway IP, Witte ON. Trop2 identifies a subpopulation of murine and human prostate basal cells with stem cell characteristics. *Proc Natl Acad Sci USA*. 2008;105:20882–20887.
30. Goldstein AS, Drake JM, Burnes DL, et al. Purification and direct transformation of epithelial progenitor cells from primary human prostate. *Nat Protoc*. 2011;6:656–667.
31. Brown MD, Gilmore PE, Hart CA, et al. Characterization of benign and malignant prostate epithelial Hoechst 33342 side populations. *Prostate*. 2007;67:1384–1396.
32. Hu WY, Shi GB, Hu DP, Nelles JL, Prins GS. Actions of estrogens and endocrine disrupting chemicals on human prostate stem/progenitor cells and prostate cancer risk. *Mol Cell Endocrinol*. 2012;354:63–73.
33. Greathouse KL, Bredfeldt T, Everitt JJ, et al. Environmental estrogens differentially engage the histone methyltransferase EZH2 to increase risk of uterine tumorigenesis. *Mol Cancer Res*. 2012;10:546–557.
34. Ince BA, Montano MM, Katzenellenbogen BS. Activation of transcriptionally inactive human estrogen receptors by cyclic adenosine 3',5'-monophosphate and ligands including antiestrogens. *Mol Endocrinol*. 1994;8:1397–1406.
35. Soto AM, Lin TM, Justicia H, Silvia RM, Sonnenschein C. An “in culture” bioassay to assess the estrogenicity of xenobiotics. In: Colborn T, Clement C, eds. *Chemically Induced Alterations in Sexual Development: The Wildlife/Human Connection*. Princeton, NJ: Princeton Scientific Publishing; 1992:295–309.
36. Taylor JA, Vom Saal FS, Welshons WV, et al. Similarity of bisphenol A pharmacokinetics in rhesus monkeys and mice: relevance for human exposure. *Environ Health Perspect*. 2011;119:422–430.
37. Levin ER. Minireview: Extranuclear steroid receptors: roles in modulation of cell functions. *Mol Endocrinol*. 2011;25:377–384.
38. Smith S, Neaves W, Teitelbaum S. Adult versus embryonic stem cells: treatments. *Science*. 2007;316:1422–1423; author reply 1422–1423.
39. Shelby M. *NTP-CERHR Monograph on the Potential Human Reproductive and Developmental Effects of Bisphenol A*. Bethesda, MD: National Institutes of Health; 2008. NIH publication 08–5994.
40. Rochester JR. Bisphenol A and human health: a review of the literature. *Reprod Toxicol*. 2013;42:132–155.
41. Vandenberg LN, Maffini MV, Wadia PR, et al. Exposure to environmentally relevant doses of the xenoestrogen bisphenol-A alters development of the fetal mouse mammary gland. *Endocrinology*. 2007;148:116–127.
42. Walker CL, Ho SM. Developmental reprogramming of cancer susceptibility. *Nat Rev Cancer*. 2012;12:479–486.
43. Okada M, Makino A, Nakajima M, Okuyama S, Furukawa S, Furukawa Y. Estrogen stimulates proliferation and differentiation of

- neural stem/progenitor cells through different signal transduction pathways. *Int J Mol Sci*. 2010;11:4114–4123.
44. Chamorro-García R, Kirchner S, Li X, et al. Bisphenol A diglycidyl ether induces adipogenic differentiation of multipotent stromal stem cells through a peroxisome proliferator-activated receptor gamma-independent mechanism. *Environ Health Perspect*. 2012;120:984–989.
  45. Baik I, Devito WJ, Ballen K, et al. Association of fetal hormone levels with stem cell potential: evidence for early life roots of human cancer. *Cancer Res*. 2005;65:358–363.
  46. Yang L, Luo L, Ji W, et al. Effect of low dose bisphenol A on the early differentiation of human embryonic stem cells into mammary epithelial cells. *Toxicol Lett*. 2013;218:187–193.
  47. Sui Y, Ai N, Park SH, et al. Bisphenol A and its analogues activate human pregnane X receptor. *Environ Health Perspect*. 2012;120:399–405.
  48. Delfosse V, Grimaldi M, Pons JL, et al. Structural and mechanistic insights into bisphenols action provide guidelines for risk assessment and discovery of bisphenol A substitutes. *Proc Natl Acad Sci USA*. 2012;109:14930–14935.
  49. Watson CS, Alyea RA, Jeng YJ, Kochukov MY. Nongenomic actions of low concentration estrogens and xenoestrogens on multiple tissues. *Mol Cell Endocrinol*. 2007;274:1–7.
  50. Le Romancer M, Poulard C, Cohen P, Sentis S, Renoir JM, Corbo L. Cracking the estrogen receptor's posttranslational code in breast tumors. *Endocr Rev*. 2011;32:597–622.
  51. Cha TL, Zhou BP, Xia W, et al. Akt-mediated phosphorylation of EZH2 suppresses methylation of lysine 27 in histone H3. *Science*. 2005;310:306–310.
  52. Belcher SM, Chen Y, Yan S, Wang HS. Rapid estrogen receptor-mediated mechanisms determine the sexually dimorphic sensitivity of ventricular myocytes to 17 $\beta$ -estradiol and the environmental endocrine disruptor bisphenol A. *Endocrinology*. 2012;153:712–720.
  53. Vinas R, Watson CS. Mixtures of xenoestrogens disrupt estradiol-induced non-genomic signaling and downstream functions in pituitary cells. *Environ Health*. 2013;12:26.
  54. Soriano S, Alonso-Magdalena P, Garcia-Arevalo M, et al. A Rapid insulinotropic action of low doses of bisphenol-A on mouse and human islets of Langerhans: role of estrogen receptor  $\beta$ . *PLoS One*. 2012;7:e31109.
  55. Xu X, Ye Y, Li T, et al. Bisphenol-A rapidly promotes dynamic changes in hippocampal dendritic morphology through estrogen receptor-mediated pathway by concomitant phosphorylation of NMDA receptor subunit NR2B. *Toxicol Appl Pharmacol*. 2010;249:188–196.
  56. Pennie WD, Aldridge TC, Brooks AN. Differential activation by xenoestrogens of ER $\alpha$  and ER $\beta$  when linked to different response elements. *J Endocrinol*. 1998;158:R11–R14.
  57. Li Y, Burns KA, Arao Y, Luh CJ, Korach KS. Differential estrogenic actions of endocrine-disrupting chemicals bisphenol A, bisphenol AF, and zearalenone through estrogen receptor  $\alpha$  and  $\beta$  in vitro. *Environ Health Perspect*. 2012;120:1029–1035.
  58. Birnbaum LS, Fenton SE. Cancer and developmental exposure to endocrine disruptors. *Environ Health Perspect*. 2003;111:389–394.
  59. Dekant W, Völkel W. Human exposure to bisphenol A by biomonitoring: methods, results and assessment of environmental exposures. *Toxicol Appl Pharmacol*. 2008;228:114–134.
  60. Schönfelder G, Wittfoht W, Hopp H, Talsness CE, Paul M, Chahoud I. Parent bisphenol A accumulation in the human maternal-fetal-placental unit. *Environ Health Perspect*. 2002;110:A703–A707.
  61. Fénelon P, Déchaux H, Harthe C, et al. Unconjugated bisphenol A cord blood levels in boys with descended or undescended testes. *Hum Reprod*. 2012;27:983–990.
  62. Edlow AG, Chen M, Smith NA, Lu C, McElrath TF. Fetal bisphenol A exposure: concentration of conjugated and unconjugated bisphenol A in amniotic fluid in the second and third trimesters. *Reprod Toxicol*. 2012;34:1–7.



Members receive *Endocrine Daily Briefing*, an email digest of endocrinology-related news selected from thousands of sources.

[www.endo-society.bulletinhealthcare.com](http://www.endo-society.bulletinhealthcare.com)

